communications biology

Article

https://doi.org/10.1038/s42003-024-06893-0

Oral microbial diversity in 18th century African individuals from South Carolina

Check for updates

Raquel E. Fleskes[1,2] ✉, Sarah J. Johnson[3,4], Tanvi P. Honap[3,4], Christopher A. Abin[3,4], Joanna K. Gilmore[2,5], La'Sheia Oubré[2], Wolf D. Bueschgen[6], Suzanne M. Abel[6], Ade A. Ofunniyin[2,5,8], Cecil M. Lewis[3,4] ✉ & Theodore G. Schurr[2,7] ✉

As part of the Anson Street African Burial Ground Project, we characterized the oral microbiomes of twelve 18th century African-descended individuals (Ancestors) from Charleston, South Carolina, USA, to study their oral health and diet. We found that their oral microbiome composition resembled that of other historic (18th-19th century) dental calculus samples but differed from that of modern samples, and was not influenced by indicators of oral health and wear observed in the dentition. Phylogenetic analysis of the oral bacteria, *Tannerella forsythia* and *Pseudoramibacter alactolyticus*, revealed varied patterns of lineage diversity and replacement in the Americas, with the Ancestors carrying strains similar to historic period Europeans and Africans. Functional profiling of metabolic pathways suggested that the Ancestors consumed a diet low in animal protein. Overall, our study reveals important insights into the oral microbial histories of African-descended individuals, particularly oral health and diet in colonial North American enslavement contexts.

Dental calculus, or mineralized dental plaque, has become an important resource for understanding the evolution of oral microbes[1]. Dental calculus forms consistently throughout an individual's lifetime on the supra- or subgingival surfaces of the teeth[2–4]. The calcium phosphate mineral structure persists in archaeological contexts, preserving biomolecules such as DNA, proteins, metabolites, and microfossils[5,6]. The preservation of dental calculus in the archaeological record further allows for a geo-spatial and temporal assessment of microbial variation in the human oral cavity.

Previous studies have highlighted differences in oral microbial composition and abundance in relation to diet[7,8] and the environment[9,10] in humans, as well as differences in oral micriobiota between humans and non-human primates[11–13]. Recent research has also demonstrated that the oral microbial communities identified in human dental calculus samples are largely similar and conserved through time[14–17]. Yet, individual microbes show evidence of strain replacement and lineage diversification associated with human migrations[17–20]. Notably, lineages of oral microbes such as *Tannerella forsythia* associated with pre-European contact American populations have been identified, with these differing from those found in post-contact, historic, and modern American populations[18,21].

Investigating how past human migrations have shaped oral microbiome composition and diversity is important for understanding their potential impact on present-day oral health disparities. One of the largest population movements in recorded history involved the forced enslavement and transportation of over 15 million persons from the African continent across the Atlantic Ocean[22]. The Trans-Atlantic Slave Trade fed the system of extractive colonialism driven by European imperialist desires for dominance and wealth, as well as religious and racial superiority[23–25]. These practices resulted in over 300,000 African persons being forcibly brought to eastern North America between the 16th and 18th centuries alone[23,26,27]. Enslaved persons endured horrendous conditions in the Middle Passage, and many thousands of lives were lost during their transportation to the Americas[27]. Individuals sold to European-American enslavers were forced to perform domestic and manual labor, sowing the economic and social foundations of colonial America on the basis of race[28]. Within this history, evidence of daily resistance in enslavement conditions have been recorded in first-person oral and written accounts[29–31], as well as demonstrated in mortuary practices[32] and foodways, including diet and food preparation techniques[33].

Examining the lived history of enslaved persons in direct conversation with descendant communities and/or other racial, cultural, geographic, and spiritual community stakeholders is of paramount importance[34]. In parallel with movements in Indigenous data sovereignty and bioethics[35,36], these

[1]Department of Anthropology, Dartmouth College, Hanover, NH, USA. [2]The Anson Street African Burial Ground Project, Mount Pleasant, SC, USA. [3]Laboratories of Molecular Anthropology and Microbiome Research (LMAMR), University of Oklahoma, Norman, OK, USA. [4]Department of Anthropology, University of Oklahoma, Norman, OK, USA. [5]Department of Sociology and Anthropology, College of Charleston, Charleston, SC, USA. [6]Charleston County Coroner's Office, North Charleston, SC, USA. [7]Department of Anthropology, University of Pennsylvania, Philadelphia, PA, USA. [8]Deceased: Ade A. Ofunniyin
✉e-mail: raquel.e.fleskes@dartmouth.edu; cecilmlewis@gmail.com; tgschurr@sas.upenn.edu

discussions have shaped contemporary conversations surrounding consent and the role of community engagement in ancient DNA (aDNA)[37–39] and microbiome studies[40–42]. Such discussions help to foster scientific accountability by making projects attuned to the priorities of impacted communities, particularly those of descendant community members. When done in collaboration, paleogenomics and microbiome research can offer crucial insights into the histories and lived experiences of subaltern communities, including aspects such as geographic origins, biological relationships, diet, and disease, which are often not well documented.

The Anson Street African Burial Ground (ASABG) Project draws from these theoretical frameworks to investigate the lives of 36 individuals of African descent that were found in downtown Charleston, South Carolina, USA. Dr. Ade Ofunniyin and the Gullah Society, Inc. (now the ASABG Project) set up a community-based initiative to understand the history of these 36 Ancestors (collectively referred to as 'The 36' or 'The Anson Street Ancestors'; the word 'Ancestors' was chosen by the community as an honorary signifier of their connection with the living). Over the course of the ASABG Project, we held a series of *Community Conversation* events, conducted educational outreach with local schools and universities, and created opportunities for arts programming to create space for expression and reflection[43]. Persons who attended our *Community Conversation* events wanted to understand the demographic profiles, relatedness, lived experiences, dietary habits, and health of the Ancestors. These activities motivated the creation of a Naming Ceremony, during which the 36 Ancestors were bestowed honorary names, instead of burial numbers, which are used in this text (see Fleskes et al. [44]. and Gilmore et al. [43]. for more details). The Ancestors were reburied in May 2019 on the grounds of their original resting place during a Reinterment Ceremony as an act of celebration and remembrance.

Thus, with community support, we undertook a multi-method investigation combining aDNA, isotopic, archaeological, and archival research. Our research indicated the individuals had primarily African genomic ancestry and were interred between 1760-1790 C.E (Supplementary Note 1)[44,45]. Chromosomal sex was assigned based on the presence of XY or XX sex chromosome data, revealing that both women and men were present in the burial ground[45].

Here, we report the findings from our study of the oral microbiomes of the Anson Street Ancestors using an aDNA and shotgun metagenomics approach grounded within a community engagement framework. We evaluated the preservation and authenticity of ancient oral microbial communities and characterized the relationship between dental pathologies and oral microbiome profiles. We also assessed differences in oral microbiome composition of the Ancestors and other ancient and modern populations using publicly available oral metagenomic data. In addition, we reconstructed the genomes of two oral bacteria, *Tannerella forsythia* and *Pseudoramibacter alactolyticus*, to investigate patterns of strain diversity and replacement in relationship to large-scale forced population migrations of the Trans-Atlantic Slave Trade and European colonialism. We further investigated dietary intake through functional profiling of metabolic pathways associated with different diets. Overall, our findings provide important insights into the oral health, makeup of oral microbial communities, and the evolution of oral taxa in the context of the African Diaspora.

Results and discussion

Presence of dental calculus and authentication of historic oral microbiomes

Dental calculus deposits were obtained from the teeth of 14 Ancestors, which included incisors, canines, premolars, and molars (Table 1; Supplementary Fig. 1; Supplementary Data 1). In cases where a limited amount of calculus was available, deposits from multiple teeth were collected.

We were able to successfully generate double-stranded DNA libraries partially treated with uracil-DNA-glycosylase (UDG) from dental calculus samples of 12 Ancestors. DNA libraries were shotgun-sequenced, generating between 17,090,464 to 51,541,395 raw reads (Supplementary Data 1). More than 80% of reads were kept following trimming, quality-filtering, and merging, resulting in 13,773,352 to 49,449,332 reads.

To estimate the endogenous human DNA content in the dental calculus samples, the processed reads were mapped to the human reference genome (hg19) (Supplementary Data 2). This resulted in 5067 to 58,170 unique mapped reads, with average fragment lengths between 56-92 base pairs (bp). Extraction and library negative controls contained 33 to 1152 unique reads mapping to the human genome. In all, the percentage of endogenous human DNA content in the Ancestors' samples ranged from 0.02–0.16%.

Human DNA damage patterns were assessed using MapDamage[46]. The majority of the Ancestors' samples had 2.72–7.21% of 5' terminal nucleotides with C-to-T misincorporations and 2.65–7.96% of 3' terminal nucleotides with G-to-A misincorporations (Supplementary Data 2;

Table 1 | Demographic profiles and tooth sampling of the Anson Street Ancestors

Name	ID	Demographics			Dental Calculus Sampling	
		Chromosomal Sex Estimation*	Genomic Ancestry Estimation*	Osteological Age Estimation	Single or Multiple Teeth Sampled	Teeth Sampled
Banza	CHS01	XY	African	Young Adult	Single	LI_1
Lima	CHS03	XY	African	Middle Adult	Single	RP_1
Anika	CHS10	N/A	African	N/A	Single	LM^1
Zimbu	CHS13	XY	African	Middle Adult	Single	LP_2
Juba	CHS14	XY	African	Middle Adult	Single	LP^1
Nina	CHS20	XX	African	Adolescent	Multiple	RP^2, RM^1, RM^2, RM^3
Kwebena	CHS21	N/A	African	Middle Adult	Single	RM^1
Lisa	CHS22	XY	African	Young Adult	Single	RM_1
Risu	CHS26	XY	African	Adult	Multiple	LI_1, RI_1, Maxillary Right Incisor, Premolar
Amina	CHS27	N/A	African	Adult	Single	LC^1
Kidzera	CHS28	N/A	African	Juvenile	Single	deciduous RC_1
Pita	CHS29	XY	African	Adult	Single	RP^2
Tima	CHS31	XX	African	Adult	Multiple	RP^1, RP^2, LP^1
Isi	CHS36	XX	African	Adult	Single	RC^1

Chromosomal sex and ancestry estimation derived from autosomal data published in Fleskes et al. [45]. Osteological age estimates were published in Fleskes et al. [44]. Honorary names of the Ancestors are provided in italics.

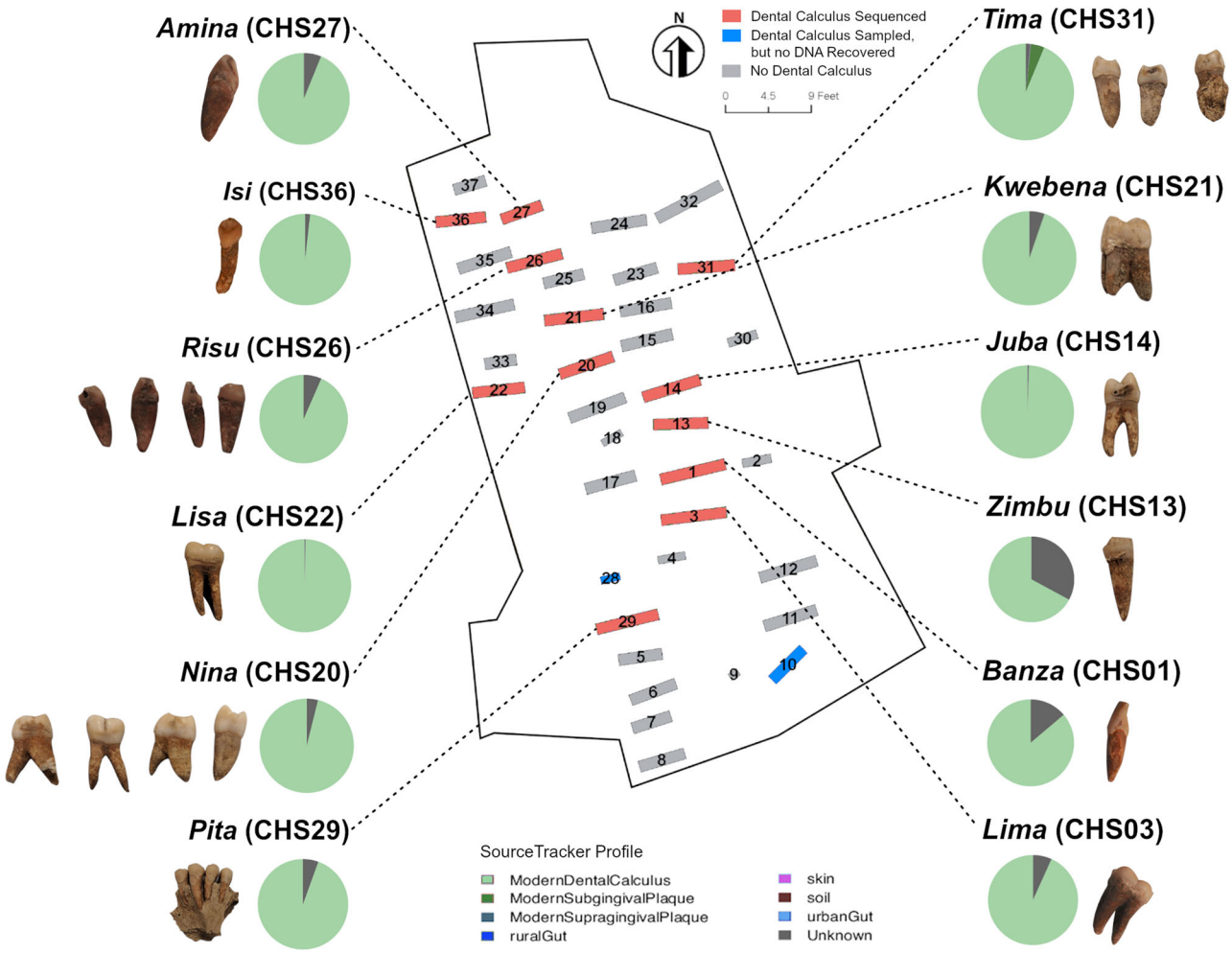

Fig. 1 | The Anson Street African Burial Ground site displaying burial numbering and dental calculus information. The Ancestors from whom dental calculus was sampled and sequenced are highlighted in red, and those where dental calculus was sampled but were not sequenced due to low recovery are highlighted in blue. The Ancestors with no dental calculus are denoted in grey. The tooth or teeth with dental calculus deposits that were collected from each Ancestor are shown. Pie charts display the results from the SourceTracker analysis. The original site map was published in Fleskes et al. [44].

Supplementary Fig. 2). Samples from three Ancestors (*Zimbu* [CHS13], *Nina* [CHS20], and *Kwebena* [CHS21]) did not show damage patterns indicative of aDNA, although the mean fragment lengths of the human DNA were in the expected size range (<100 bp). Due to the possibility of low-level contamination from modern sources, we excluded data from these individuals from statistical comparisons of microbial taxonomic and functional profiles. Prior to further analyses, reads mapping to the human genome were removed from the Ancestors' metagenomes, resulting in 13,734,044 to 49,410,798 reads across all samples, hereafter referred to as 'analysis-ready' reads.

We conducted microbial species-level taxonomic profiling by screening the analysis-ready reads using MetaPhlAn4[47] and estimated the proportion of potential contaminants through SourceTracker[48] analysis. Modern calculus, plaque, feces, skin, and soil samples were used as 'sources'. For all 12 Ancestors, the majority of reads present in the libraries were attributed to microbes found in oral sources (Fig. 1; Supplementary Data 3).

Characterization of oral microbial profiles

A total of 239 microbial species were identified in the Ancestors' calculus samples using MetaPhlAn4 (Supplementary Data 4–5). Most of these species are characteristically found in mature oral biofilms such as dental calculus[16]. While no microbial taxa were detected in the laboratory controls, we filtered out taxa whose origin could not be authenticated as being oral, as well as those found in only one sample prior to downstream analyses (Supplementary Data 6). After filtering, we visualized the 25 most abundant species using a heatmap (Fig. 2A).

The most abundant oral bacterial species identified was an unclassified Firmicutes bacterium (SGB71327), followed by *Methanobrevibacter oralis* and *Actinomyces dentalis*. The presence of a high number of unclassified Firmicutes species highlights the need for deeper sequencing of oral taxa and refinement of genomic databases to better characterize oral microbiomes. We also detected taxa known to be early colonizers of oral biofilms[49–51], such as *Actinomyces* and *Streptococcus*[47,49,50]. Bridging species, such as *Fusobacterium nucleatum*, which represent a transition from the primarily aerobic early colonizers to facultative anaerobic late colonizers, were also identified[51–53]. Late colonizers, including *Tannerella* and *Porphyromonas* species and *Parvimonas micra*, were found in most of the Ancestors[49,52,53]. Known opportunistic pathogens such as *Treponema denticola*, *Tannerella forsythia*, and *Porphyromonas gingivalis*, which are collectively known as the 'Red Complex' and associated with periodontal disease[54] were also detected. The unique MetaPhlAn4 profile observed in *Zimbu* [CHS13] resulted from the lack of identifiable taxa (Fig. 2B).

Correlation between oral health and oral microbial communities

To understand the relationship between the oral metagenomic profiles and oral pathologies, we first examined the Ancestors' complete dental arcade and the individual tooth and/or teeth sampled for dental calculus (Table 2). Carious lesions were the most commonly identified, with 10 Ancestors

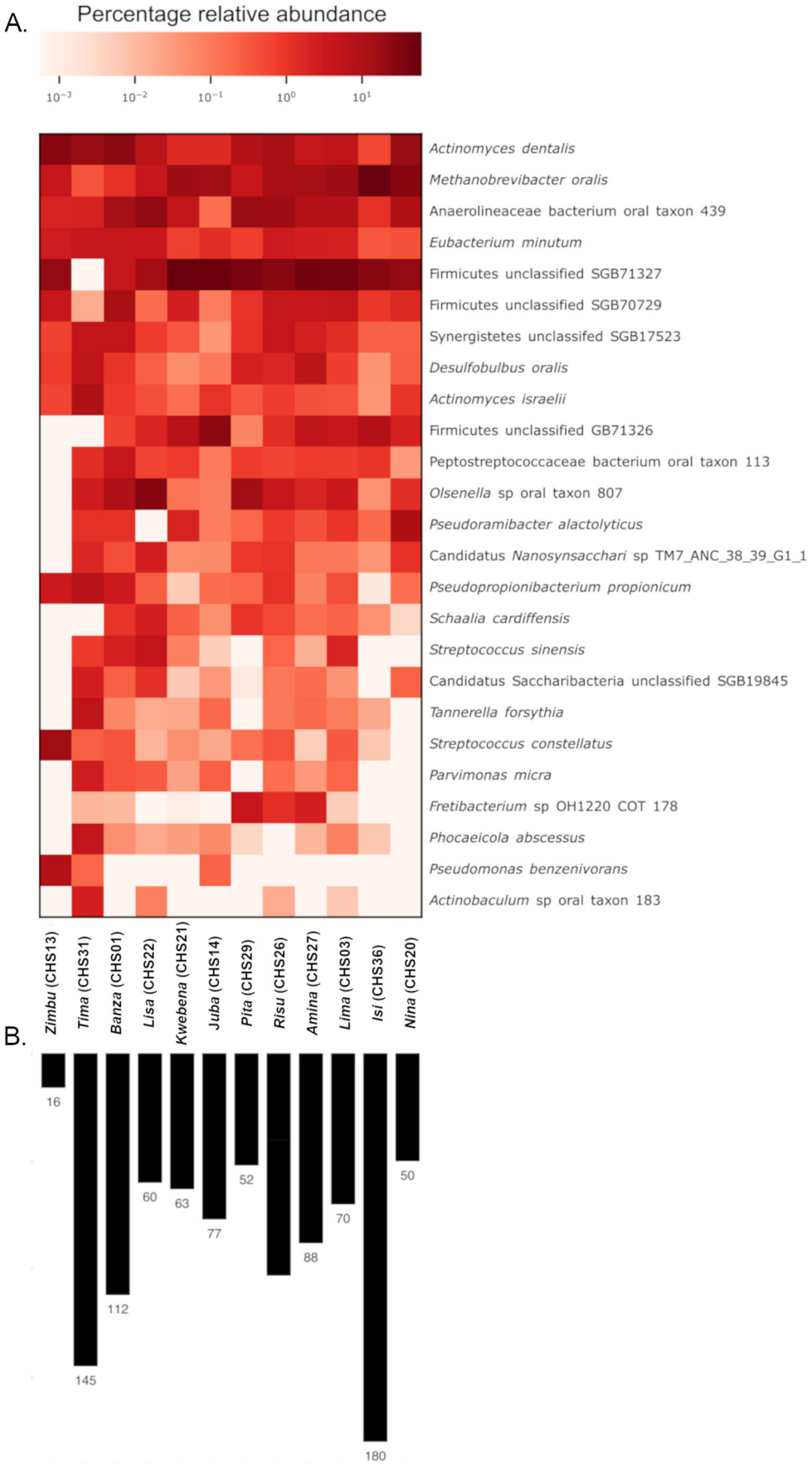

Fig. 2 | MetaPhlAn4 results. A A heatmap showing the 25 most abundant species. **B** The histogram indicates total number of taxa identified for each Ancestor.

Table 2 | Dental pathologies and other notable dental features observed in the 14 Anson Street Ancestors analyzed in this study

Name	ID	Source	Oral Health / Infection					Wear				Enamel Defects		Other		
			Abscess	Antemortem Tooth Loss	Caries	Infection at Root Tip	Periodontitis	Generalized Wear	Occlusal Attrition	Pipe Facet Wear	Tooth Modification	Enamel Hypoplasia	Staining	Malocclusion	Supra-eruption	Tooth Fracture
Banza	CHS01	Sampled Tooth/Teeth														
		Total Dental Arcade							X							
Lima	CHS03	Sampled Tooth/Teeth														
		Total Dental Arcade			X				X							
*Anika**	CHS10	Sampled Tooth/Teeth			X											
		Total Dental Arcade			X						X		X			X
Zimbu	CHS13	Sampled Tooth/Teeth			X			X								
		Total Dental Arcade	X	X	X	X		X				X				
Juba	CHS14	Sampled Tooth/Teeth			X											
		Total Dental Arcade	X	X	X	X	X	X				X				
Nina	CHS20	Sampled Tooth/Teeth														
		Total Dental Arcade						X								
Kwebena	CHS21	Sampled Tooth/Teeth														
		Total Dental Arcade		X	X		X			X			X			
Lisa	CHS22	Sampled Tooth/Teeth						X								
		Total Dental Arcade	X	X	X	X		X				X	X			
Risu	CHS26	Sampled Tooth/Teeth			X											
		Total Dental Arcade			X											
Amina	CHS27	Sampled Tooth/Teeth														
		Total Dental Arcade			X											
*Kidzera**	CHS28	Sampled Tooth/Teeth														
		Total Dental Arcade														
Pita	CHS29	Sampled Tooth/Teeth														
		Total Dental Arcade	X	X	X		X			X		X	X		X	
Tima	CHS31	Sampled Tooth/Teeth			X											
		Total Dental Arcade	X		X					X			X			
Isi	CHS36	Sampled Tooth/Teeth														
		Total Dental Arcade														

The symbol "*" indicates that the calculus extracted from these individuals did not yield enough DNA for sequencing. Honorary names of the Ancestors are provided in italics. The symbol "X" indicates the feature is noted.

displaying one or more lesions. Other pathological changes included those associated with oral health and infection (abscess, antemortem tooth loss, caries, infection, and periodontitis), wear (generalized, occlusal attrition, pipe facet, and tooth modification), enamel defects (enamel hypoplasia and staining), and supra-eruption and tooth fractures. These pathologies were also previously observed in the Ancestors lacking dental calculus, except for malocclusion[44].

When analyzing the complete dental arcade, we found that the Ancestors with dental calculus deposits either displayed very few or multiple oral pathologies. Individuals with multiple pathologies were mostly associated with oral health or generalized wear (Table 2; Supplementary Fig. 3A). Analysis of the individual teeth with dental calculus deposits indicated that six Ancestors had dental pathologies, classified as either dental caries or occlusal wear (Table 2; Supplementary Fig. 3B). These observations align with previous conclusions from a complete assessment of the 36 Ancestors, suggesting they had overall poor oral health[44].

Next, we conducted principal component analysis (PCA) to assess correlations between dental pathology metadata variables and the oral microbiome composition of the Ancestors (Supplementary Data 6). Bi-plots displaying the PCA loadings (Fig. 3A) were generated to illustrate how different variables affect sample distribution in the PCA space[55]. For the Ancestors, negative PCA loadings were primarily influenced by unclassified Firmicutes species and

Methanobrevibater oralis (Fig. 3B). Positive PCA loadings were characterized by anaerobic or facultative anaerobic taxa, and driven by the presence of *Actinomyces dentalis*, *Olsenella*, and *Pseudopropionibacterium* (Fig. 3B).

Subsequently, we examined whether there was a relationship between the number or type of oral pathologies and the oral microbiome profiles. We integrated the comparative oral pathology metadata with the previously generated PCA distributions and conducted PERMANOVA association testing to assess their significance (Supplementary Fig. 4; Supplementary Table 1). None of the dental pathology metadata variables were found to be significant. However, no Ancestors with dental calculus deposits contained a complete dental arcade, thereby limiting the completeness of this assessment.

Following this methodological approach, we investigated how migration might affect oral metagenomic composition by integrating previously published strontium isotopic data indicating the likely place of childhood residence[44]. Of the authenticated oral metagenomic profiles from the Anson Street Ancestors, only *Banza* [CHS01], a young male, likely resided in West or West Central Africa during his childhood and lived some of his adult life in North America. However, PERMANOVA testing between PCA distributions and residency patterns did not show any significant associations (Supplementary Fig. 4A; Supplementary Table 1). Thus, additional data are needed to determine how residency may affect oral microbiome composition throughout a person's lifetime.

These findings contribute to the ongoing discussion about the links between oral health and microbial community structure in dental calculus[14,15,18,56]. We observed numerous taxa associated with oral infection and pathogenicity in the dental calculus of Ancestors with poor oral health, consistent with previous studies[56]. However, our results did not reveal a direct relationship between specific microbial community profiles and oral pathology, as seen in other studies[15,18]. Together, these results highlight the limitations of using microbial community profiles of archaeological dental calculus to directly estimate oral health of past populations.

Comparative analysis of dental calculus microbiome composition

To compare the oral microbial composition of the Anson Street Ancestors with other dental calculus samples, we selected comparative data based on geographic location, time period, sample number, and availability and conducted a PCA using the MetaPhlAn4-based relative abundances of detected species (Supplementary Data 7–8). The dental calculus samples from the Ancestors grouped on the right side of the plot with positive PC1 values but displayed variability along the second PC dimension (Fig. 4A). Notably, they aligned with other archaeological individuals from the historic period in Asia (Japan) and Africa (Morocco, South Africa) along the positive PC1 axis. Conversely, modern European samples (Spain) exhibited negative PC1 values to the left on the PCA plot. PERMANOVA analysis confirmed significant differences based on site, time period, and location (Supplementary Table 2).

To investigate whether the PCA distributions were influenced by the number of identified species, we colored PCA points by species number (Fig. 4B; Supplementary Data 9). Our results revealed that dental calculus samples with fewer identified species appeared to cluster along the positive PC1 axis. By contrast, modern dental calculus samples had a relatively higher number of identified species and were positioned away from archaeological samples. Samples with very few identified species (< 25) clustered in the middle of the PCA. PERMANOVA analysis suggested this pattern was not significant (Supplementary Table 2). Several factors, including DNA preservation and the lack of appropriate reference genomes in databases, may contribute to fewer species being identified in certain ancient dental calculus samples[15].

We conducted a bi-plot analysis to examine the impact of species assemblages on PCA distributions, focusing on the top ten taxa influencing positive and negative loadings for the first dimension (Fig. 4C). The species influencing positive loadings in this analysis were observed in a previous bi-plot featuring only the Anson Street Ancestors (Fig. 3). In contrast, the majority of species contributing to negative PC1 dimensions were rarely detected in the Anson Street Ancestors but more commonly found in modern dental calculus samples. These taxa, such as *Ottowia*, *Neisseria sicca*, and others, represent a spectrum of both early and late colonizer species commonly encountered in the oral cavity[50,57,58]. Differences in species composition between the historic and modern dental calculus samples may also be influenced by modern oral hygiene practices, which can prevent dental plaque buildup and result in higher levels of early colonizer taxa[1], or a number of other factors related or unrelated to host ecology[15].

Genome reconstruction of oral bacteria, *Tannerella forsythia* and *Pseudoramibacter alactolyticus*

A total of 173 taxa identified using MetaPhlAn4 (Supplementary Data 10) were targeted for microbial genome reconstruction using a reference-based mapping approach[18]. We were able to authenticate the recovery of partial or near-complete ancient genomes for several species of interest, including *Tannerella forsythia*, *Treponema denticola*, *Streptococcus constellatus*, and *Pseudoramibacter alactolyticus* (Supplementary Fig. 5A–D). Excluding strains that were recovered at low-coverage or those with high heterozygosity values indicative of the presence of multiple strains within a dental calculus sample restricted our phylogenetic analyses to two species, *T. forsythia* and *P. alactolyticus*. The former is an opportunistic oral pathogen long-associated with periodontal disease, whereas the latter is an understudied oral microbe commonly found in some ancient dental calculus samples and is a primary endodontic pathogen in modern contexts[56,59]. We were able to successfully reconstruct and authenticate a partial *T. forsythia* strain from *Tima* [CHS31] and two partial *P. alactolyticus* strains from *Lima* [CHS03] and *Nina* [CHS20].

Previous research on *T. forsythia* indicates that the human-associated strains fall into two major lineages whose histories are entangled with the impact of European colonialism[18,21]. Lineage 1 appears to be limited to the pre-contact era Americas, as it has only been recovered from dental calculus samples from pre-contact Indigenous individuals from Mexico[21], and Wichita Ancestors from Oklahoma, USA[18]. Lineage 2 strains have been identified in historic era (18th-19th century) individuals from Europe and South Africa, and in modern individuals from the USA, Europe, and Asia, suggesting that it is the major lineage prevalent worldwide today and likely replaced Lineage 1 after European contact[18]. Our phylogenetic analysis based on alignments of homozygous SNPs across the *T. forsythia* genome placed *Tima's* [CHS31] strain in Lineage 2, although its relationship to other Lineage 2 strains could not be assessed due to limited bootstrap support (Fig. 5, Supplementary Fig. 6). The placement of *Tima's* [CHS31] strain suggests that historic period African persons carried strains similar to historic populations outside of North America.

Our phylogenetic analysis of the species *P. alactolyticus* using alignments of homozygous SNPs across the genome (Fig. 6, Supplementary Fig. 7) and a curated set of essential genes (Supplementary Figs. 8, 9) identified two major lineages in this species. Lineage 1 is present in the Americas and Asia and includes strains from pre-contact era Indigenous individuals from Mexico and Wichita Ancestors from the USA, historic era (17th–19th century) Japanese individuals, and modern individuals from China and the USA, with the latter being the reference strain for this species. Lineage 2 includes strains from individuals from ancient Egypt, historic era (18th–19th century) South Africa, and modern Europe, and an environmental isolate from Italy. Removing the environmental strain did not affect the tree structure, supporting its place in Lineage 2. Strains from *Lima* [CHS03] and *Nina* [CHS20] both belonged to Lineage 2, which is otherwise not found in individuals from the Americas. Within Lineage 2, *Nina's* [CHS20] strain was closely related to a historic era strain from the U.K., whereas *Lima's* [CHS03] strain was closely related to a historic era strain from South Africa, suggesting it was likely brought over to the Americas during the Trans-Atlantic Slave Trade.

Analysis of enamel strontium isotopes for *Lima* [CHS03] and *Nina* [CHS20] indicated that these Ancestors were probably not born in Africa,

A.

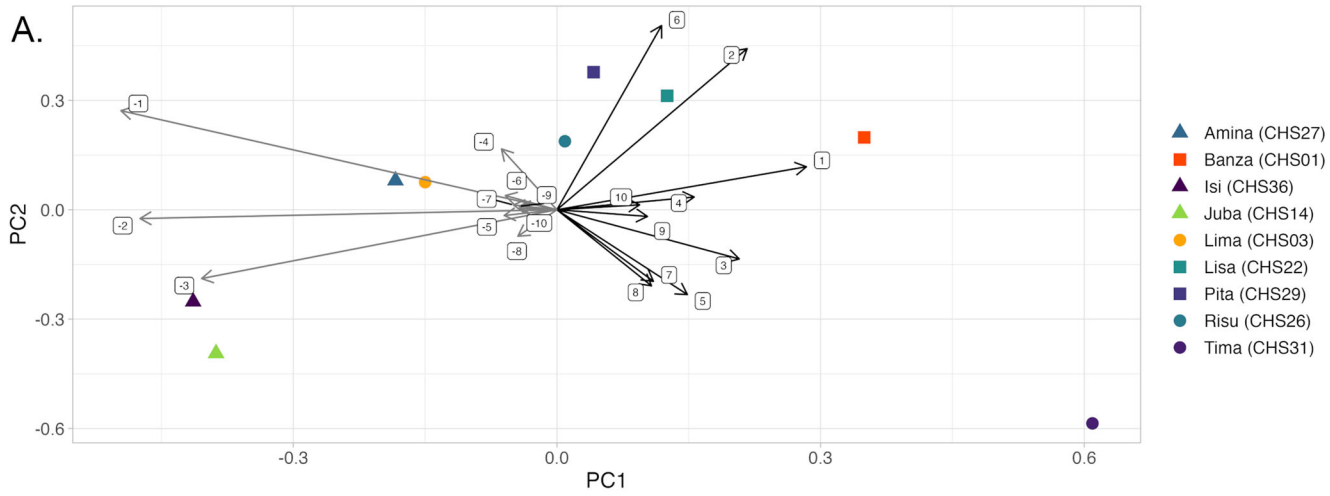

B.

Order	PC1	Species
-1	-0.495987	*GGB51111_SGB71327*
-2	-0.47427	*Methanobrevibacter_oralis*
-3	-0.404165	*GGB51110_SGB71326*
-4	-0.062999	*Fretibacterium_sp_OH1220_COT_178*
-5	-0.060012	*Actinomyces_oricola*
-6	-0.058687	*Desulfomicrobium_orale*
-7	-0.049414	*Synergistes_jonesii*
-8	-0.044323	*Mogibacterium_timidum*
-9	-0.043012	*Treponema_SGB69452*
-10	-0.04261	*Streptococcus_sanguinis*

Order	PC1	Species
1	0.283871	*Actinomyces_dentalis*
2	0.216435	*Olsenella_sp_oral_taxon_807*
3	0.207466	*Pseudopropionibacterium_propionicum*
4	0.156218	*GGB10852_SGB17523*
5	0.148466	*Actinomyces_israelii*
6	0.11907	*Anaerolineaceae_bacterium_oral_taxon_439*
7	0.109797	*Phocaeicola_abscessus*
8	0.107596	*Tannerella_forsythia*
9	0.103049	*Desulfobulbus_oralis*
10	0.094108	*Eubacterium_minutum*

Fig. 3 | Bi-Plot analysis of the MetaPhlAn4 mean relative abundances for the Anson Street Ancestors. A Bi-Plot analysis, with black arrows representing the top 10 species with the highest PCA loadings, and grey arrows representing the top 10 species with negative PCA loadings. **B** The table of species corresponding to the arrows, matching the arrow numbers.

and thus likely represent second or later generations of African descendants whose ancestors were brought to the Americas through forced migration[44]. Despite their local origin, these Ancestors do not carry strains of *T. forsythia* and *P. alactolyticus* native to North America which could have been acquired through contact with Indigenous communities in the vicinity or from the local environment. In *Lima's* [CHS03] case, at least one of these oral strains likely originated in Africa.

The finding of strains closely aligned with those from historic and modern African or European populations suggests the Ancestors either acquired them from African persons through vertical transmission over generations through caregivers[60,61] or via frequent contact with other persons of African descent and/or enslavers or other persons of European descent. For the latter, this could possibly manifest through cultural practices or demographic processes[17]. The exact transmission dynamics can be difficult to disentangle in archaeological contexts, since oral strains can be acquired through both vertical and horizontal transmission over the course of an individual's lifetime[62]. However, the competitive interplay between different strains may result in discordant evolutionary outcomes for different species within the same oral ecology.

Our phylogenetic analysis indicates differences in the evolutionary trajectories of two oral microbes, *T. forsythia* and *P. alactolyticus*, in the Americas. In case of *T. forsythia*, the non-American lineage seems to have replaced the pre-existing American lineage after contact, whereas, in the case of *P. alactolyticus*, the pre-existing American lineage persists today. However, wider sampling and genomic data for modern strains from the Americas will help provide a better understanding of how contact with Europeans and the subsequent forced Trans-Atlantic migrations influenced the strain dynamics of different oral microbes.

Analysis of microbial functional profiles in the context of diet

Although dietary practices can influence oral microbiome composition[63–68], recent literature has highlighted the complexities of identification and authentication of dietary DNA in low-coverage ancient oral metagenome data[16,69]. We attempted to detect eukaryotic DNA sequences in the Ancestors' oral metagenomes by screening the analysis-ready reads using Kraken2[70] and a custom database comprising prokaryotic, mitochondrial, and plastid genomes. However, we were unable to authenticate damage patterns for these eukaryotic DNA sequences, preventing direct determination of dietary constituents (Supplementary Fig. 10). Therefore, we employed an indirect approach to infer dietary components using an analysis of microbial gene functions related to carnivorous and herbivorous diets[71].

We used HUMAnN3[47] to characterize microbial functional profiles of the Anson Street Ancestors, along with those of pre-contact era agricultural Wichita Ancestors from the USA, historic era individuals from the Radcliffe Infirmary, United Kingdom, and modern Spanish individuals to contextualize possible dietary constituents across subsistence practices. We assessed the presence of 40 enzymes previously identified[71] in gut metagenomes to be differentially abundant depending on diet (Supplementary Data 11)[69]. Resource availability strongly drives the functional potential of a microbiome, with functional diversity often being decoupled from taxonomic diversity in metabolically niche environments[72–74], supporting the assumption that enzymes linked to meat consumption in gut microbiomes can be identified in oral microbiomes, regardless of the originating body site.

Of these 40 enzymes, we identified 38 that could be linked to 66 KEGG Orthologous (KO) categories measuring plant or meat consumption. A total of 31 KO categories were present at greater than two counts per million (cpm) in at least 75% of dental calculus samples. KO categories measuring plant consumption did not show significant variability across the

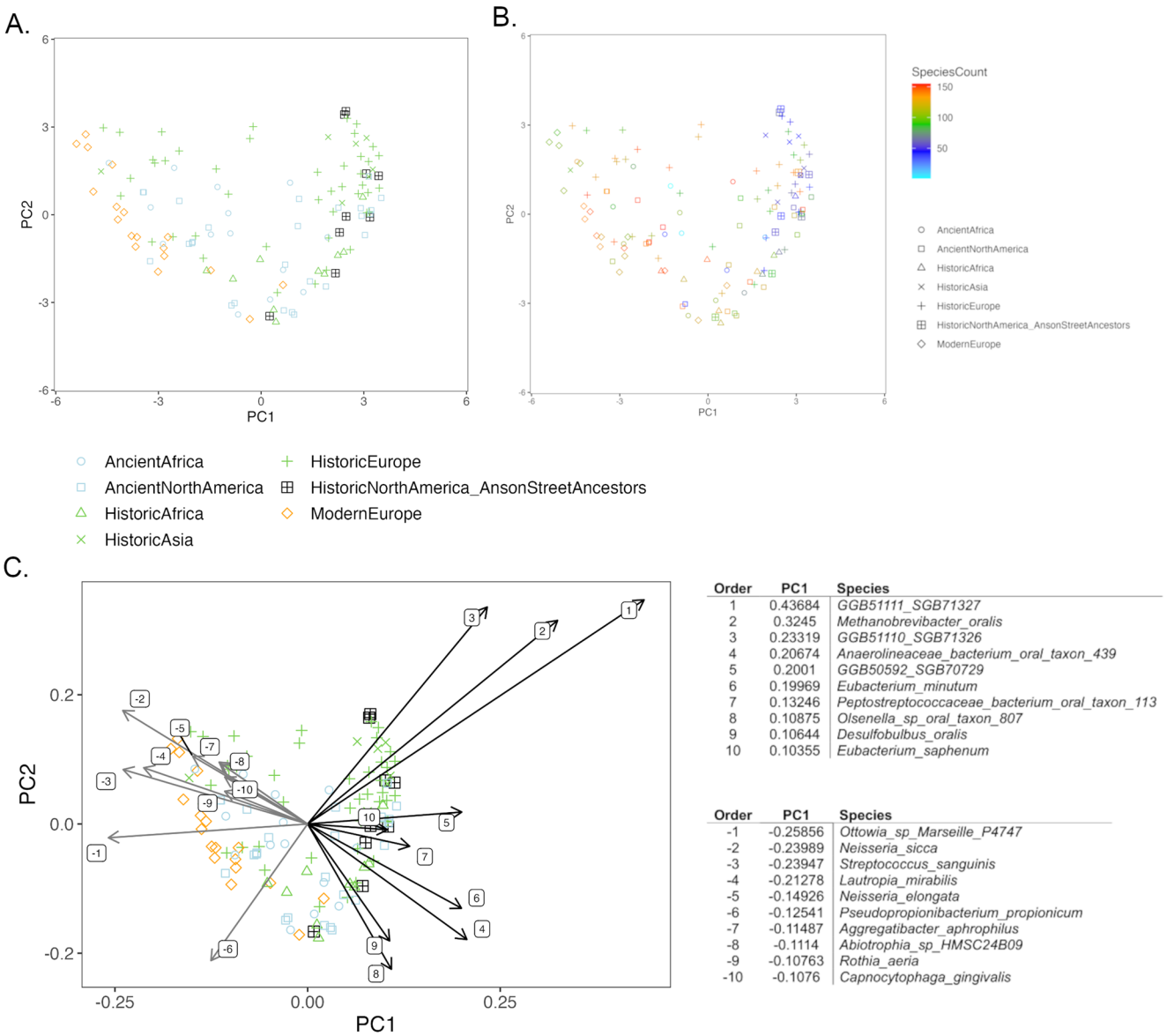

Order	PC1	Species
1	0.43684	*GGB51111_SGB71327*
2	0.3245	*Methanobrevibacter_oralis*
3	0.23319	*GGB51110_SGB71326*
4	0.20674	*Anaerolineaceae_bacterium_oral_taxon_439*
5	0.2001	*GGB50592_SGB70729*
6	0.19969	*Eubacterium_minutum*
7	0.13246	*Peptostreptococcaceae_bacterium_oral_taxon_113*
8	0.10875	*Olsenella_sp_oral_taxon_807*
9	0.10644	*Desulfobulbus_oralis*
10	0.10355	*Eubacterium_saphenum*

Order	PC1	Species
-1	-0.25856	*Ottowia_sp_Marseille_P4747*
-2	-0.23989	*Neisseria_sicca*
-3	-0.23947	*Streptococcus_sanguinis*
-4	-0.21278	*Lautropia_mirabilis*
-5	-0.14926	*Neisseria_elongata*
-6	-0.12541	*Pseudopropionibacterium_propionicum*
-7	-0.11487	*Aggregatibacter_aphrophilus*
-8	-0.1114	*Abiotrophia_sp_HMSC24B09*
-9	-0.10763	*Rothia_aeria*
-10	-0.1076	*Capnocytophaga_gingivalis*

Fig. 4 | Comparative PCA analysis of the Metaphalan4 mean relative abundances at the species level. A PCA depicting the Anson Street Ancestors and comparative reference populations. The legend and color symbols are denoted on the bottom of the plot and are additionally shared with subpanel C. **B** A PCA analysis, with coloring representing the number of identified species. Legend symbols are denoted in the same subpanel. **C** A Bi-Plot analysis, with arrows denoting the top 10 species with the highest and lowest PCA loadings shown in the corresponding table. Legend and color symbols are shown above the plot.

comparative populations (p-value > 0.07), although there was a distinct difference in the abundance of KO categories associated with meat consumption (p-value < 8×10^{-12}) (Fig. 7; Supplementary Fig. 11). Overall, the Anson Street Ancestors had an average abundance of 40.8 cpm of meat-associated KO categories compared to 67.8 cpm (p-value < 9×10^{-6}) for the Wichita, 60.4 cpm (p-value < 7×10^{-5}) for the historic Radcliffe, and 105.6 cpm (p-value < 9×10^{-11}) in the modern Spanish individuals. This finding implies that, in comparison to the other analyzed populations, the Ancestors did not consume large amounts of animal protein.

The lower consumption of animal protein by individuals of African descent in enslavement conditions is supported by historical, archaeological, and isotopic research[75]. Archival records indicate that diets primarily consisted of vegetables and grains, many grown by the enslaved individuals themselves, and supplemented with locally foraged wild game and fish[76]. Faunal analyses from archaeological sites in North America and the Caribbean also support these findings, displaying evidence of consumption of wild game and fish, and fewer prime cuts of stock animals like cows[77–79]. Nitrogen stable isotope ratios further indicated a diet lower in meat or possibly higher in wild game and fish for enslaved individuals[80,81]. An ongoing analysis of nitrogen isotopes for the Anson Street Ancestors will assist in evaluating the link between diet and microbial functional profiles. Additionally, analyzing samples from non-enslaved populations in South Carolina is crucial for discerning whether the observed microbial pattern is due to enslavement conditions or instead represents a regional pattern of dietary practices.

Conclusions

Employing a community–engaged approach, this study characterized the oral microbiome profiles of the Anson Street Ancestors to understand their lived histories, health, and diet. This study also represents the largest assemblage of oral microbiome data from colonial era African individuals published to date. Our analysis revealed no strong associations between oral microbiome composition, oral health, and childhood residency, suggesting the relative stability of oral community structure during a person's lifetime. Additionally, the Ancestors' oral community profiles were similar to those of other archaeological individuals, but differed from those of individuals

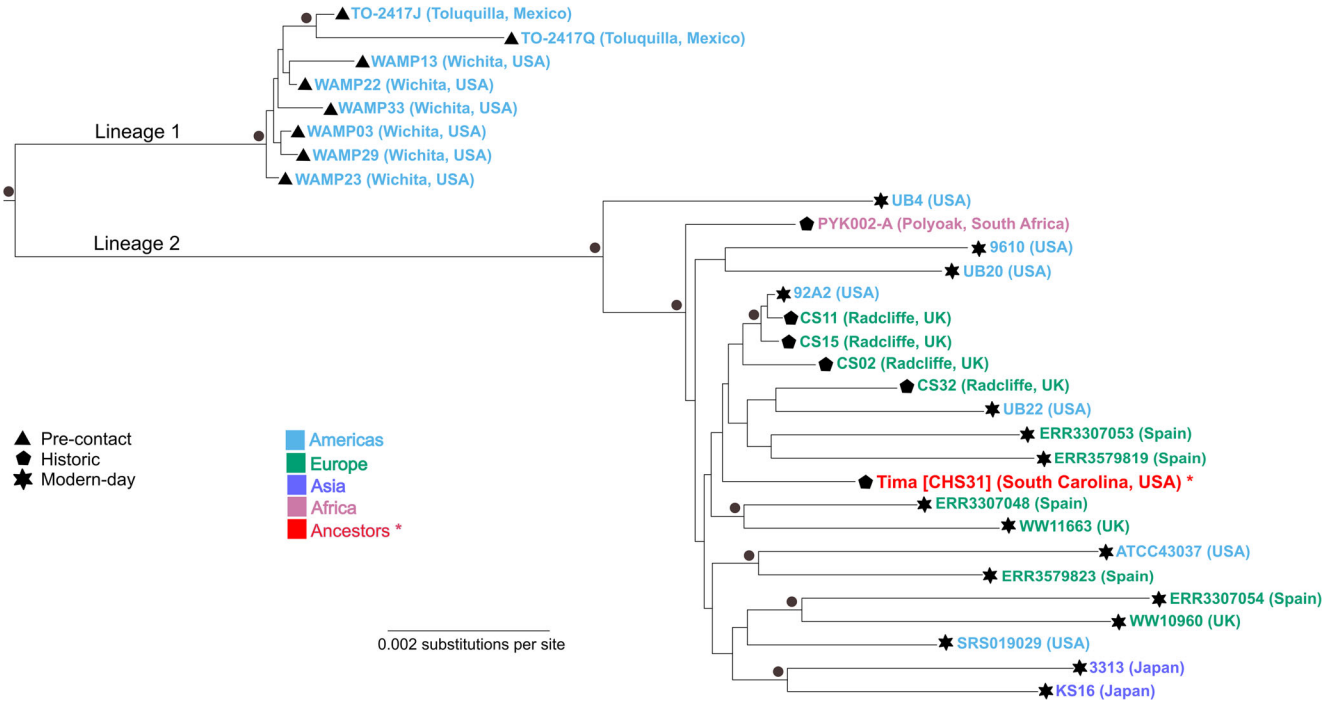

Fig. 5 | Maximum Likelihood tree of *Tannerella forsythia* strains. An alignment of 26,922 homozygous, bi-allelic SNPs was used. The tree was built using IQ-TREE and the K3PU + F + ASC + R2 model. The tree was rooted using canine *T. forsythia* strains. Brown circles indicate branches with greater than 95% bootstrap support, estimated using 1000 ultrafast bootstraps. Strains are color-coded based on location, symbols are used to denote temporal context, and the country of origin is shown in parentheses. The strain reconstructed from Ancestor *Tima* [CHS31], is colored in red.

from the modern era, indicating that oral communities have shifted over time. Moreover, our investigation into the phylogenies of *Tannerella forsythia* and *Pseudoramibacter alactolyticus* revealed that the lineages of these species carried by the Ancestors correspond to those found in European and African populations.

These findings offer valuable insights into oral microbial histories which, in turn, inform our larger understanding of oral health and diet for enslaved African or African descendant populations in the U.S. South. Ultimately, this study significantly contributes to our growing understanding of the oral microbial histories, shedding light on their oral health and dietary patterns, as well as emphasizes the pivotal role of community engagement in oral microbiome research.

Methods

Ethics and community engagement

The ASABG Project is a community-based effort to understand the lives of 36 Ancestors of African descent in conversation and collaboration with people living in the Charleston region[43]. Public presentations describing what can be learned from the analysis of dental calculus were given during community events prior to starting laboratory analyses to ensure adequate time for people to learn and provide feedback about the study. We made additional public presentations to share the progression of preliminary findings, as well the final results presented here. The contents of this manuscript were subsequently shaped following these conversations, which primarily concerned questions about oral health and diet of the Ancestors.

Oral pathological analysis

Oral pathologies and modifications were assessed for all individuals with intact dentition as outlined in Fleskes et al. [44]. Specifically, features associated with oral health (carious lesions, abscesses, tooth loss, and infection), wear (generalized, occlusal, and modifications), and enamel defects (enamel hypoplasia and staining) were noted for each tooth containing dental calculus and the available dental arcade for the individual.

Dental calculus sampling

Calculus samples were collected from the teeth of 14 Ancestors in May 2019 at Brockington & Associates in Mount Pleasant, South Carolina (Supplementary Fig. 1) following guidelines from Velsko and Warinner[83]. Dental scrapers were decontaminated between each sample by wiping all tools with 10% bleach followed by 70% ethanol. Sterile gloves were worn and replaced between each sampling. Calculus samples were stored at room temperature until DNA extraction. The calculus samples collected ranged between 0.2–10.6 mg in weight (Supplementary Data 1). Samples from multiple teeth were combined for three Ancestors in order to have sufficient amounts for DNA extraction.

Shotgun sequencing

All laboratory work was conducted at the Laboratories of Molecular Anthropology and Microbiome Research, University of Oklahoma (Norman, USA), following established workflows for aDNA research[84]. The calculus samples were irradiated for 1 minute on each side using a UV Crosslinker (VWR) and washed with 1 mL of 0.5 M EDTA for 15 minutes to remove surface contaminants. A fresh solution of 1 mL 0.5 M EDTA solution and 100 µL Proteinase K (Qiagen) was added, and the calculus samples were allowed to decalcify over a 4-day period. Following calculus decalcification and digestion, a MinElute column-based purification (Qiagen) was conducted, as described in Ozga et al. [85], with DNA being eluted in 60 µL Buffer EB (Qiagen) pre-heated to 65°C. An extraction blank (PCR-grade water, GeneMate) was processed along with the calculus samples to monitor for laboratory contamination. DNA extracts were quantified using the Qubit High Sensitivity dsDNA Assay (Life Technologies).

A 30 µL aliquot of DNA extract was partially treated with uracil-DNA-glycosylase[86] and built into a double-stranded DNA library as given in Carøe et al. [87]. A library blank (PCR-grade water, GeneMate) was processed during library preparation to monitor for laboratory contamination. Libraries were indexed with two unique eight bp barcodes using the Kapa HiFi Uracil+ enzyme (Kapa Biosystems) and purified using the Sera-Mag SpeedBead clean-up protocol (Thermo Scientific), as described in Honap et al. [18].

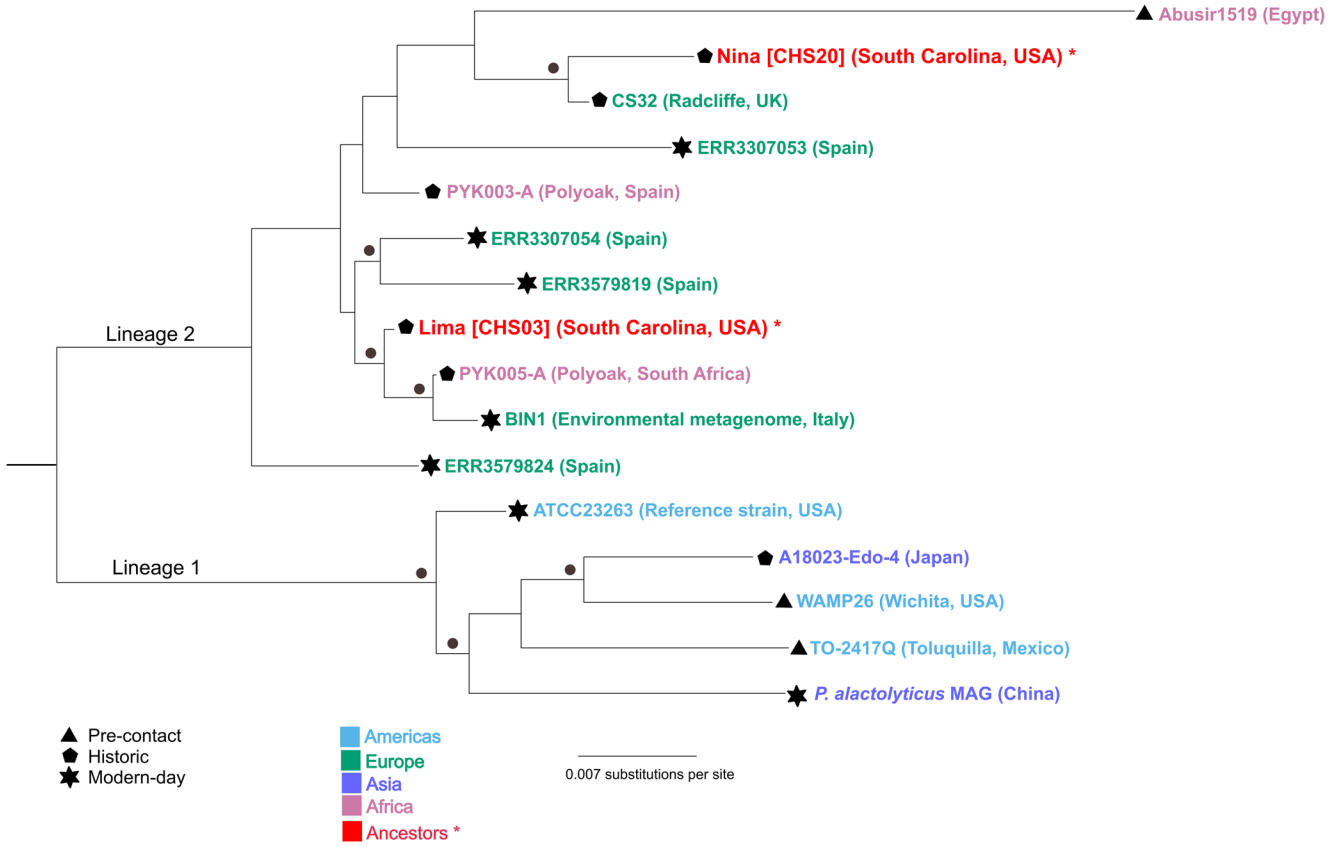

Fig. 6 | Maximum Likelihood tree of *Pseudoramibacter alactolyticus* strains. An alignment of 3,083 homozygous, bi-allelic SNPs with a maximum of 10% missing data was used. The tree was built with IQ-TREE using the K3Pu +F + ASC + R2 model. A strain reconstructed from a wild-borne chimpanzee was used as the outgroup. Brown circles indicate branches with greater than 95% bootstrap support from 1,000 ultrafast bootstrap replicates. The color of each strain corresponds to geographic origin and the symbols equate to temporal context. Strains reconstructed from Ancestors *Lima* [CHS03] and *Nina* [CHS20] are colored in red.

Library fragment size and concentration was assessed using the D1000 assay on the TapeStation (Agilent).

Library samples from two Ancestors showed negligible proportions of DNA fragments in the targeted size range of 150–500 bp and were thus excluded from further processing. The remaining 12 libraries were pooled in equimolar amounts. The resulting pool was concentrated using the Vacufuge (Eppendorf) to a volume of 30 µL and used as input for the PippinPrep (Sage Systems) to perform size-selection for a target range of 150–500 bp to remove adapter dimers. The resulting eluate was shotgun-sequenced using the Illumina HiSeq X and paired-end 2 × 150 bp sequencing at Admera Health (New Jersey, USA).

Sequence read processing

Raw reads were processed using AdapterRemoval v2.3.3[88] with the following options: –trimns, –trimqualities, –minquality 30, and –minlength 30. Reads with a minimum overlap of 10 bases were merged.

Human genome filtering

To assess endogenous human DNA content, filtered, merged reads were aligned to the human reference genome (hg19) using Bowtie v2.4.1[89], keeping both aligned and unaligned reads. Using SAMTools v1.16.1[90], the resulting SAM files were converted to BAM format, sorted, and split into BAM files of either aligned or unaligned reads. For the hg19-aligned BAM file, duplicate reads were removed using DeDup v0.12.8[91], and MapDamage v2.2.1[46] was used to assess DNA damage patterns. The BAM files containing reads not aligned to hg19 were converted to FASTQ files using the bam2FastQ tool from BamUtil v1.0.15[92]; these reads, hereafter referred to as 'analysis-ready' reads, were used for subsequent analysis.

Microbial taxonomic screening and authentication

Species-level taxonomic screening was conducted using the analysis-ready reads and MetaPhlAn v4.0.1[47] with the –minreadlength 30 option. The 25 most abundant microbial species, in terms of average relative abundance, were visualized using a heatmap generated with hclust2.py[93]. The origin of the detected species was cross-validated using the Human Oral Microbiome Database[94], NCBI Taxonomy Browser, and other publicly available sources. Species likely to be of environmental origin were removed.

SourceTracker v2.0.1[48] was used to assess oral microbiome preservation and potential extraneous contamination by converting the species-level relative abundance tables from MetaPhlAn4 into counts. The Ancestors' calculus samples were used as the 'sink', whereas samples of modern dental calculus[14], sub- and supra-gingival plaque[95], feces from traditional hunter-gatherer and urban industrialized populations[64,96,97], skin[98], and soil[99] were processed using the same parameters and used as 'sources'. Gibbs sampling was performed using the following parameters: source and sink rarefaction depth = 20,000, alpha1 = 0.01, and alpha2 = 1.0. The results were visualized as pie charts generated using a custom script.

Comparative datasets

To assess temporal and geographic changes in oral microbial diversity and composition, we used the Ancient Metagenome Directory[100] to select publicly available oral metagenomic datasets. These ranged from ancient to modern contexts, including modern Spain[14,16], historic Asia[20], historic Africa[16], historic United Kingdom[14], ancient Africa[16,101] and pre-contact North America[18] (Supplementary Data 7). For this study, time period

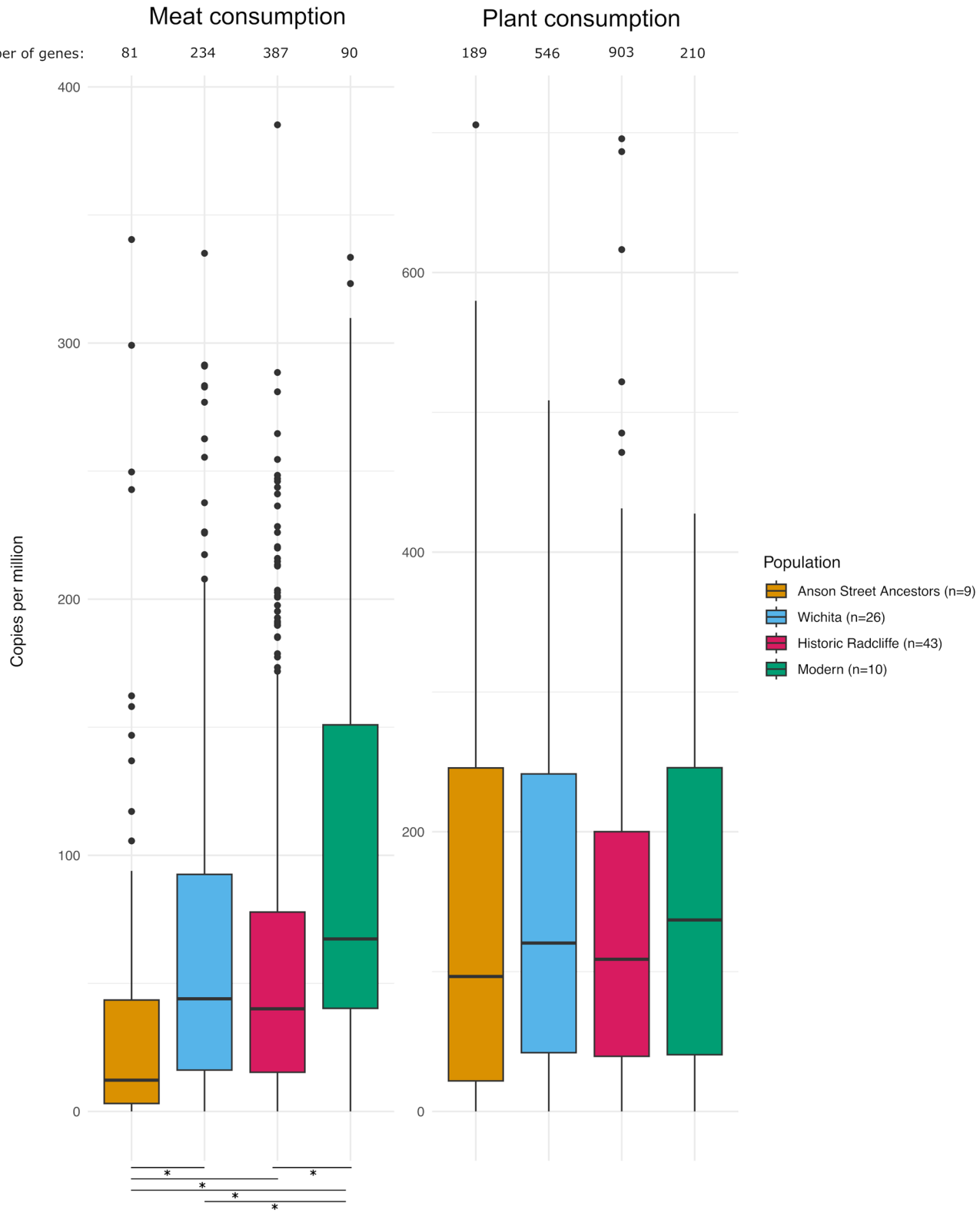

Fig. 7 | Functional analysis of animal protein consumption. HUMAnN3 gene family abundances aggregated based on high-meat or high-plant consumption. Pairwise Wilcoxon rank sum tests for significance with p-values < 0.05 are indicated below the graph by asterisks. The number of genes in each population are displayed above each bar and detailed statistics are outlined in Supplementary Data 18.

designations for modern contexts include samples collected from present day populations, historic period from individuals living 300–200 YA, post-contact around 700 YA, and ancient from 14,500–1600 YA. All datasets were processed using similar parameters as the Ancestors' dental calculus samples.

Principal component analysis

To identify correlations between sample metadata and taxonomic composition, we carried out PCA using R v.4.3.1. The MetaPhlAn4 species level table was filtered to include only those species present at greater than 0.05% relative abundance in at least 10% of samples. We used the phyloseq[102] and

mix0mics packages[103] and applied a centered-log ratio (CLR) transformation suitable for compositional data. PCA plots were generated using ggplot2[104]. Euclidean distances were calculated from the first principal component using the vegan package[105]. The Adonis2 function was used to perform PERMANOVA testing to generate R2, F, and P values between the generated distance matrices and sample metadata. Bi-plots were generated following Velsko et al. [15], with the top 10 species showing the highest and lowest negative loadings identified and plotted using a correction factor in ggplot2[104].

Microbial genome reconstruction

Analysis-ready reads were mapped to the reference genomes of 173 microbial species identified using MetaPhlAn4[93] (Supplementary Data 10), using BWA aln v.0.7.15-r1140[106] with the following parameters: -l 1024, -q 37, -n 0.1. The resulting SAM files were converted to the BAM format, unmapped reads were filtered out, and the BAM files were sorted using SAMTools v1.16.1[90]. DeDup v0.12.8[91] was used to remove duplicate reads. MapDamage v2.2.1[46] was used to assess DNA damage patterns and rescale the BAM files to reduce quality scores of likely damaged positions. Qualimap v.2.2.1[107] was used to generate coverage statistics.

Variant calling was conducted if the mapped reads were authenticated using MapDamage, and at least 30% of the reference genome was covered at least five-fold. Prior to variant calling, the trimBam option in BamUtil v1.0.15[92] was used to remove two bases from each end of the reads to avoid false variant calls due to the presence of DNA damage. The resulting clipped BAM file was used as input for SAMTools mpileup with the -aa option to output all sites. A VCF file was generated using VarScan v2.3.9[108] mpileup2cns with the following parameters: minimum coverage = 5, minimum reads to call a variant = 3, minimum average quality = 37, minimum variant frequency = 0.2, minimum frequency for homozygotes = 0.9, p-value = 1, and strand filter = 0.

Microbial phylogenetic analysis

To ascertain the phylogenetic relationships of *T. forsythia* and *P. alactolyticus* strains reconstructed from the Ancestors, publicly available genomic data for ancient dental calculus and modern oral sources (calculus and plaque) were used as comparative datasets. Additionally, complete or contig-level genomes were acquired from the National Center for Biotechnology Information (NCBI). For the latter, paired-end reads were simulated using wgsim[109] with the following parameters: -1 = 150, -2 = 150, -d = 100, -r = 0, -R = 0, -X = 0, and -e = 0. For all datasets, reads were mapped to the appropriate reference genomes and variant calling was conducted in a manner similar to that for the Ancestors.

Samples were included in the phylogenetic analysis provided they fulfilled four criteria: (1) more than 30% of the genome was recovered at a minimum of five-fold coverage; (2) the ratio of heterozygous SNPs to homozygous SNPs was less than 1, signifying presence of a single, dominant strain; (3) they exhibited characteristic damage patterns for ancient DNA; and (4) genomes could be retrieved from comparative datasets. Summary statistics related to mapping and variant calling are provided in Supplementary Data 12 and 13. While we were able to reconstruct and authenticate partial or near-complete genomes of several oral species from the Ancestors' samples, we focused our phylogenetic analysis only on *Tannerella forsythia* and *Pseudoramibacter alactolyticus* due the parameters described above.

To build the alignment, VCF files for selected samples were merged using bcftools v1.5[110] with the -m all option. For SNP-based phylogenies, bcftools view was used to output only bi-allelic SNPs (options: –type snps, -m 2, -M 2). Insertion-deletions and SNPs occurring in repetitive regions, rRNAs, tRNAs, mobile and insertion elements, and phage-related genes were removed using vcftools v.0.1.17[111]. The genomic regions excluded for *P. alactolyticus* are presented in Supplementary Data 14, whereas those for *T. forsythia* are described in Honap et al. [18]. FASTA files containing the final SNP alignments were generated from the VCF file using a publicly available script[112] and used for building phylogenetic trees. Maximum Likelihood SNP trees were built using IQTREE v1.6.12[113] with the following options: -m MFP, -bnni, and -alrt. Branch support was assessed by performing 5000 replicates of ultrafast bootstrap approximation[114].

For *P. alactolyticus*, a multi-gene phylogeny was built based upon an alignment of 205 genes (Supplementary Data 15) annotated as "essential" in this reference genome according to The Bacterial and Viral Bioinformatics Resource Center[115]. A Maximum Likelihood gene tree was built using IQTREE and similar parameters as given before. Maximum Parsimony trees for both SNP- and gene-based alignments were built using MEGA-X[116], with the SPR algorithm and 1000 bootstrap replicates. All trees were visualized using FigTree (http://tree.bio.ed.ac.uk/software/figtree/).

Functional analysis

Analysis-ready reads were screened for metabolic potential using HUMAnN v3.6[47]. This pipeline taxonomically assessed the metagenomes using MetaPhlAn4[93] (database mpa_vJan21_CHOCOPhlAnSGB_202103) and characterized gene family groups through pangenome nucleotide alignment and translated alignment to the UniRef50[117] database to produce taxonomically informed functional profiles. The output includes gene families reported in reads per kilobase (RPK) and pathways defined by MetaCyc[118] reported as the total abundance of genes catalyzing reported reactions. Gene families were used for comparative analyses and merged with those acquired from pre-European contact Wichita samples[18], historic samples from the Radcliffe Infirmary (United Kingdom) and modern samples from Spain[14]. Gene families reported as RPK, or relative gene copy number, in each community were normalized to copies per million (cpm) to account for any variation in sequencing depth and unmapped categories were excluded (Supplementary Data 19). Normalized gene families were regrouped to provide KEGG orthologous (KO) categories[119–121], excluding ungrouped gene families, and unstratified tables were filtered to include only those functional categories present at a minimum of 2 cpm in at least 75% of samples.

Dietary assessment

An initial direct assessment of dietary constituents through screening for eukaryotic DNA was attempted using Kraken2[70] with a custom database of mitochondrial and plastid genomes from NCBI, as well as representative fungal, viral, and protozoan genomes from NCBI and bacterial and archaeal genomes from the Genome Taxonomy Database (GTDB) v214.1[122–125] to ensure a diverse reference database for competitive read mapping[126]. The database was built and the samples assessed using default parameters (k-mer length of 35 and minimizer length of 31). Kraken2 classification was followed by Bracken v2.6 analysis, a Bayesian re-estimation tool that accompanies Kraken tools and predicts abundance at specified taxonomic levels[127]. The Bracken database was built with both a k-mer size and read length of 35. BWA v0.7.17[106] was then used to align the analysis-ready reads to the 20 most abundant eukaryotic species detected using Bracken. Coverage, read length, and damage profiles of alignments with >500 unique reads were used to assess the validity of the presence of eukaryotic dietary constituents (Supplementary Data 16-17; Supplementary Fig. 10).

For the indirect assessment, the annotated KEGG abundance tables were screened for evidence of dietary constituents. KO categories with Enzyme Commission (E.C.) numbers enriched in herbivorous and carnivorous mammalian populations[71] were extracted to infer meat consumption (Supplementary Data 11). Kruskal-Wallis tests for statistical significance and Pairwise Wilcoxon rank sum tests with false discovery rate correction[128] were performed on each category in R and p-values were reported (Supplementary Data 18).

Data availability

In line with previous agreements to prevent commercialization of the genomic data following wishes of community stakeholders (see Fleskes et al. [45]), all human genomic data have been filtered from the oral metagenomic dataset. The filtered metagenomic dataset is publicly accessible via the Sequence Read Archive (PRJNA1037120). Source data underlying figures and tables can be

found in Supplementary Data and Tables. Scripts used for bioinformatic analyses are publicly available on Github (https://github.com/sarah9602/Anson-St-Ancestors-Oral-Microbiome) and Zenodo[82].

Received: 15 November 2023; Accepted: 13 September 2024;
Published online: 28 September 2024

References

1. Warinner, C., Speller, C., Collins, M. J. & Lewis, C. M. Ancient human microbiomes. *J. Hum. Evolution* **79**, 125–136 (2015).
2. Akcali, A. & Lang, N. P. Dental calculus: The calcified biofilm and its role in disease development. *Periodontology 2000* **76**, 109–115 (2018).
3. Fagernäs, Z. & Warinner, C. Dental Calculus. in *Handbook of Archaeological Sciences* (eds. Pollard, A. M., Armitage, R. A. & Makarewicz, C. A.) (John Wiley & Sons, 2023).
4. White, D. J. Dental calculus: Recent insights into occurrence, formation, prevention, removal and oral health effects of supragingival and subgingival deposits. *Eur. J. Oral. Sci.* **105**, 508–522 (1997).
5. Radini, A. & Nikita, E. Beyond dirty teeth: Integrating dental calculus studies with osteoarchaeological parameters. *Quat. Int.* **653–654**, 3–18 (2023).
6. Warinner, C. et al. Pathogens and host immunity in the ancient human oral cavity. *Nat. Genet.* **46**, 336–344 (2014).
7. Adler, C. J. et al. Sequencing ancient calcified dental plaque shows changes in oral microbiota with dietary shifts of the Neolithic and Industrial revolutions. *Nat. Genet.* **45**, 450–455 (2013).
8. Innocenti, G., Martino, M. E., Stellini, E., Di Fiore, A. & Quagliariello, A. Dental calculus microbiome correlates with dietary intake. *Mol. Oral Microbiol.* **38**, 189–197 (2022).
9. Li, J. et al. Comparative analysis of the human saliva microbiome from different climate zones: Alaska, Germany, and Africa. *BMC Microbiol.* **14**, 1–13 (2014).
10. Moraitou, M. et al. Ecology, not host phylogeny, shapes the oral microbiome in closely related species. *Mol. Biol. Evolution* **39**, 1–62 (2022).
11. Ozga, A. T. et al. Oral microbiome diversity in chimpanzees from Gombe National Park. *Sci. Rep.* **9**, 1–15 (2019).
12. Ottoni, C. et al. Metagenomic analysis of dental calculus in ancient Egyptian baboons. *Sci. Rep.* **9**, 1–10 (2019).
13. Li, J. et al. The saliva microbiome of Pan and Homo. *BMC Microbiol.* **13**, 204 (2013).
14. Velsko, I. M. et al. Microbial differences between dental plaque and historic dental calculus are related to oral biofilm maturation stage. *Microbiome* **7**, 1–20 (2019).
15. Velsko, I. M. et al. Ancient dental calculus preserves signatures of biofilm succession and interindividual variation independent of dental pathology. *PNAS Nexus* **1**, 1–14 (2022).
16. Fellows Yates, J. A. et al. The evolution and changing ecology of the African hominid oral microbiome. *Proc. Natl Acad. Sci. USA* **118**, 1–11 (2021).
17. Ottoni, C. et al. Tracking the transition to agriculture in Southern Europe through ancient DNA analysis of dental calculus. *Proc. Natl Acad. Sci. USA* **118**, 1–11 (2021).
18. Honap, T. P. et al. Oral metagenomes from Native American Ancestors reveal distinct microbial lineages in the pre-contact era. *Am. J. Biol. Anthropol.* **182**, 1–15 (2023).
19. Granehäll, L. et al. Metagenomic analysis of ancient dental calculus reveals unexplored diversity of oral archaeal Methanobrevibacter. *Microbiome* **9**, 1–18 (2021).
20. Eisenhofer, R., Kanzawa-Kiriyama, H., Shinoda, K. I. & Weyrich, L. S. Investigating the demographic history of Japan using ancient oral microbiota: Ancient Japanese dental calculus. *Philos. Trans. R. Soc. B: Biological Sciences* **375**, 20190578 (2020).
21. Bravo-Lopez, M. et al. Paleogenomic insights into the red complex bacteria Tannerella forsythia in Pre-Hispanic and Colonial individuals from Mexico. *Philos. Trans. R. Soc. B: Biological Sciences* **375**, 20190580 (2020).
22. *Routes to Slavery: Direction, Ethnicity, and Mortality in the Transatlantic Slave Trade*. (Routledge, London, 2013).
23. Smallwood, S. E. *Saltwater Slavery: A Middle Passage from Africa to American Diaspora*. (Harvard University Press, Cambridge, 2008).
24. Green, T. *A Fistful of Shells: West Africa from the Rise of the Slave Trade to the Age of Revolution*. (Penguin UK, 2019).
25. Cannon, K. G. Christian imperialism and the Transatlantic Slave Trade. *J. Feminist Stud. Relig.* **24**, 127–134 (2008).
26. Eltis, D. Methodology: Imputing numbers of slaves. *Slave Voyages* https://www.slavevoyages.org/voyage/about#methodology/imputing-numbers-of-slaves/14/en/ (2018).
27. Mustakeem, S. M. *Slavery at Sea: Terror, Sex, and Sickness in the Middle Passage*. (University of Illinois Press, 2016).
28. Berlin, I. *Many Thousands Gone: The First Two Centuries of Slavery in North America*. (Harvard University Press, 2009).
29. Johnson, J. M. *Wicked Flesh: Black Women, Intimacy, and Freedom in the Atlantic World*. (University of Pennsylvania Press, Incorporated, 2020).
30. Dadzie, S. *A Kick in the Belly: Women, Slavery and Resistance*. (Verso Books, 2021).
31. Robertson, N. S. *The Slave Ship Clotilda and the Making of AfricaTown, USA: Spirit of Our Ancestors*. (Bloomsbury Academic, 2008).
32. Jamieson, R. Material culture and social death: African-American burial practices. *Historical Archaeol.* **29**, 39–58 (1995).
33. Carney, J. & Rosomoff, R. N. *In the Shadow of Slavery: Africa's Botanical Legacy in the Atlantic World*. (Univ of California Press, 2009).
34. Flewellen, A. O. et al. "The Future of Archaeology Is Antiracist": Archaeology in the Time of Black Lives Matter. *Am. Antiquity* **86**, 1–20 (2021).
35. Tsosie, K. S., Begay, R. L., Fox, K. & Garrison, N. A. Generations of genomes: Advances in paleogenomics technology and engagement for Indigenous people of the Americas. *Curr. Opin. Genet. Dev.* **62**, 91–96 (2020).
36. Tsosie, K. S., Claw, K. G. & Garrison, N. A. Considering "Respect for Sovereignty" beyond the Belmont Report and the Common Rule: Ethical and legal implications for American Indian and Alaska Native Peoples. *Am. J. Bioeth.* **21**, 27–30 (2021).
37. Tsosie, K. S. et al. Ancient-DNA researchers write their own rules. *Nature* **600**, 37 (2021).
38. Fleskes, R. E. et al. Ethical guidance in human paleogenomics: New and ongoing perspectives. *Annu. Rev. Genomics Hum. Genet.* **23**, 627–652 (2022).
39. Wagner, J. K. et al. Fostering responsible research on ancient DNA. *Am. J. Hum. Genet.* **107**, 183–195 (2020).
40. Mangola, S. M., Lund, J. R., Schnorr, S. L. & Crittenden, A. N. Ethical microbiome research with Indigenous communities. *Nat. Microbiol.* **7**, 749–756 (2022).
41. Bader, A. C. et al. A relational framework for microbiome research with Indigenous communities. *Nat. Microbiol.* **8**, 1768–1776 (2023).
42. Handsley-Davis, M. et al. Microbiome ownership for Indigenous peoples. *Nat. Microbiol.* **8**, 1777–1786 (2023).
43. Gilmore, J. K., Ofunniyin, A. A., Oubré, L. O., Fleskes, R. E. & Schurr, T. G. The dead have been awakened in the service of the living" – Activist community-engaged archaeology in Charleston, SC. *Am. Antiquity* **89**, 0–0 (2024).
44. Fleskes, R. E. et al. Ancestry, health, and lived experiences of enslaved Africans in 18th century Charleston: An osteobiographical analysis. *Am. J. Phys. Anthropol.* **175**, 3–24 (2021).
45. Fleskes, R. E. et al. Community-engaged ancient DNA project reveals diverse origins of 18th-century African descendants in

Charleston, South Carolina. *Proc. Natl Acad. Sci. USA* **120**, e2201620120 (2023).
46. Jónsson, H., Ginolhac, A., Schubert, M., Johnson, P. & Orlando, L. MapDamage2.0: Fast approximate Bayesian estimates of ancient DNA damage parameters. *Bioinforma. Appl. Note* **29**, 1682–1684 (2013).
47. Beghini, F. et al. Integrating taxonomic, functional, and strain-level profiling of diverse microbial communities with bioBakery 3. *eLife* **10**, 1–42 (2021).
48. Knights, D. et al. Bayesian community-wide culture-independent microbial source tracking. *Nat. Methods* **8**, 761–765 (2011).
49. Sarkonen, N. et al. Oral colonization of Actinomyces species in infants by two years of age. *J. Dent. Res.* **79**, 864–867 (2000).
50. Zijnge, V. et al. Oral biofilm architecture on natural teeth. *PLoS ONE* **5**, e9321 (2010).
51. Welch, J. L. M., Rossetti, B. J., Rieken, C. W., Dewhirst, F. E. & Borisy, G. G. Biogeography of a human oral microbiome at the micron scale. *Proc. Natl Acad. Sci. USA* **113**, E791–E800 (2016).
52. Bradshaw, D. J., Marsh, P. D., Keith Watson, G. & Allison, C. Role of Fusobacterium nucleatum and coaggregation in anaerobe survival in planktonic and biofilm oral microbial communities during aeration. *Infect. Immun.* **66**, 4729–4732 (1998).
53. Borisy, G. G. & Valm, A. M. Spatial scale in analysis of the dental plaque microbiome. *Periodontology 2000* **86**, 97–112 (2021).
54. Socransky, S. S., Haffajee, A. D., Cugini, M. A., Smith, C. & Kent, R. L. Jr Microbial complexes in subgingival plaque. *J. Clin. Periodontol.* **25**, 134–144 (1998).
55. Gloor, G. B., Wu, J. R., Pawlowsky-Glahn, V. & Egozcue, J. J. It's all relative: Analyzing microbiome data as compositions. *Ann. Epidemiol.* **26**, 322–329 (2016).
56. Willmann, C. et al. Oral health status in historic population: Macroscopic and metagenomic evidence. *PLoS ONE* **13**, e0196482 (2018).
57. Morou-Bermudez, E., Rodriguez, S., Bello, A. S. & Dominguez-Bello, M. G. Urease and dental plaque microbial profiles in children. *PLoS ONE* **10**, e0139315 (2015).
58. Ihara, Y. et al. Identification of initial colonizing bacteria in dental plaques from young adults using full-length 16S rRNA gene sequencing. *mSystems* **4**, e00360-19 (2019).
59. Siqueira, J. F. & Rôças, I. N. Pseudoramibacter alactolyticus in primary endodontic infections. *J. Endod.* **29**, 735–738 (2003).
60. Tanner, A. C. R. et al. Similarity of the oral microbiota of pre-school children with that of their caregivers in a population-based study. *Oral. Microbiol. Immunol.* **17**, 379–387 (2002).
61. Shaw, L. et al. The human salivary microbiome Is shaped by shared environment rather than genetics: Evidence from a large family of closely related individuals. *mBio* **8**, e01237–17 (2017).
62. Kaan, A. M., Kahharova, D. & Zaura, E. Acquisition and establishment of the oral microbiota. *Periodontology 2000* **86**, 123–141 (2021).
63. Weyrich, L. S. et al. Neanderthal behaviour, diet, and disease inferred from ancient DNA in dental calculus. *Nature* **544**, 357–361 (2017).
64. Obregon-Tito, A. J. et al. Subsistence strategies in traditional societies distinguish gut microbiomes. *Nat. Commun.* **6**, 6505 (2015).
65. De Filippo, C. et al. Diet, environments, and gut microbiota. A preliminary investigation in children living in rural and Urban Burkina Faso and Italy. *Front. Microbiol.* **8**, 1979 (2017).
66. Kisuse, J. et al. Urban diets linked to gut microbiome and metabolome alterations in children: A comparative cross-sectional study in Thailand. *Front. Microbiol.* **9**, 1345 (2018).
67. Warinner, C. et al. Direct evidence of milk consumption from ancient human dental calculus. *Sci. Rep.* **4**, 1–6 (2014).
68. Gomez, A. et al. Gut microbiome of coexisting BaAka Pygmies and Bantu reflects gradients of traditional subsistence patterns. *Cell Rep.* **14**, 2142–2153 (2016).
69. Mann, A. E. et al. Do I have something in my teeth? The trouble with genetic analyses of diet from archaeological dental calculus. *Quat. Int.* **653–654**, 33–46 (2023).
70. Wood, D. E., Lu, J. & Langmead, B. Improved metagenomic analysis with Kraken 2. *Genome Biol.* **20**, 257 (2019).
71. Muegge, B. D. et al. Diet drives convergence in gut microbiome functions across mammalian phylogeny and within humans. *Science* **332**, 970–974 (2011).
72. Louca, S. et al. High taxonomic variability despite stable functional structure across microbial communities. *Nat. Ecol. Evol.* **1**, 1–12 (2016).
73. Louca, S. et al. Function and functional redundancy in microbial systems. *Nat. Ecol. Evol.* **2**, 936–943 (2018).
74. Tringe, S. G. et al. Comparative Metagenomics of Microbial Communities. *Science* **308**, 554–557 (2005).
75. Singleton, T. A. The archaeology of slavery in North America. *Annu. Rev. Anthropol.* **24**, 119–140 (1995).
76. Covey, H. C. & Eisnach, D. *What the Slaves Ate: Recollections of African American Foods and Foodways from the Slave Narratives*. (Bloomsbury Academic, 2009).
77. Wallman, D. Subsistence as transformative practice: The zooarchaeology of slavery in the colonial Caribbean. *J. Afr. Diaspora Archaeol. Herit.* **9**, 77–113 (2020).
78. Crader, D. C. Slave diet at Monticello. *Antiquity* **55**, 690–717 (1990).
79. Otto, J. S. *Cannon's Point Plantation, 1794-1860: Living Conditions and Status Patterns in the Old South*. (Elsevier, 2014).
80. France, C. A. M. et al. Stable isotopes from the African site of Elmina, Ghana and their usefulness in tracking the provenance of enslaved individuals in 18th- and 19th-century North American populations. *Am. J. Phys. Anthropol.* **171**, 298–318 (2020).
81. Mbeki, L., Kootker, L. M., Kars, H. & Davies, G. R. Sickly slaves, soldiers and sailors. Contextualizing the Cape's 18th–19th century Green Point burials through isotope investigation. *J. Archaeological Sci.: Rep.* **11**, 480–490 (2017).
82. Johnson, S., Honap, T., Fleskes, R., Lewis, C. & Schurr, T. G. Anson Street Ancestors Oral Microbiome GitHub Repository. Zenodo https://doi.org/10.5281/zenodo.13328166 (2024).
83. Velsko, I. M. & Warinner, C. Bioarchaeology of the human microbiome. *Bioarchaeology Int.* **1**, 86–99 (2017).
84. Orlando, L. et al. Ancient DNA analysis. *Nat. Rev. Methods Primers* **1**, 1 (2021).
85. Ozga, A. T. et al. Successful enrichment and recovery of whole mitochondrial genomes from ancient human dental calculus. *Am. J. Phys. Anthropol.* **160**, 220–228 (2016).
86. Rohland, N., Harney, E., Mallick, S., Nordenfelt, S. & Reich, D. Partial uracil-DNA-glycosylase treatment for screening of ancient DNA. *Philos. Trans. R. Soc. B: Biol. Sci.* **370**, 20130624 (2015).
87. Carøe, C. et al. Single-tube library preparation for degraded DNA. *Methods Ecol. Evolution* **9**, 410–419 (2018).
88. Schubert, M., Lindgreen, S. & Orlando, L. AdapterRemoval v2: Rapid adapter trimming, identification, and read merging. *BMC Res. Notes* **9**, 1–7 (2016).
89. Langmead, B. & Salzberg, S. L. Fast gapped-read alignment with Bowtie 2. *Nat. Methods* **9**, 357–359 (2012).
90. Danecek, P. et al. Twelve years of SAMtools and BCFtools. *GigaScience* **10**, 1–4 (2021).
91. Peltzer, A. et al. EAGER: Efficient ancient genome reconstruction. *Genome Biol.* **17**, 60 (2016).
92. Jun, G., Wing, M. K., Abecasis, G. R. & Kang, H. M. An efficient and scalable analysis framework for variant extraction and refinement from population-scale DNA sequence data. *Genome Res.* **25**, 918–925 (2015).
93. Blanco-Míguez, A. et al. Extending and improving metagenomic taxonomic profiling with uncharacterized species using MetaPhlAn 4. *Nat. Biotechnol.* **41**, 1633–1644 (2023).

94. Escapa, I. F. et al. New insights into human nostril microbiome from the Expanded Human Oral Microbiome Database (eHOMD): A resource for the microbiome of the human aerodigestive tract. *mSystems* **3**, e00187–18 (2018).
95. Gevers, D. et al. The Human Microbiome Project: A community resource for the healthy human microbiome. *PLoS Biol.* **10**, e1001377 (2012).
96. Sankaranarayanan, K. et al. Gut microbiome diversity among Cheyenne and Arapaho individuals from western Oklahoma. *Curr. Biol.* **25**, 3161–3169 (2015).
97. Rampelli, S. et al. Metagenome sequencing of the Hadza hunter-gatherer gut microbiota. *Curr. Biol.* **25**, 1682–1693 (2015).
98. Oh, J., Byrd, A. L., Park, M., Kong, H. H. & Segre, J. A. Temporal stability of the human skin microbiome. *Cell* **165**, 854–866 (2016).
99. Johnston, E. R. et al. Metagenomics reveals pervasive bacterial populations and reduced community diversity across the Alaska tundra ecosystem. *Front. Microbiol.* **7**, 579 (2016).
100. Fellows Yates, J. A. et al. Community-curated and standardized metadata of published ancient metagenomic samples with AncientMetagenomeDir. *Sci. Data* **8**, 1–8 (2021).
101. Neukamm, J. et al. 2000-year-old pathogen genomes reconstructed from metagenomic analysis of Egyptian mummified individuals. *BMC Biol.* **18**, 1–18 (2020).
102. McMurdie, P. J. & Holmes, S. Phyloseq: An R Package for reproducible interactive analysis and graphics of microbiome census data. *PLoS ONE* **8**, e61217 (2013).
103. Lê Cao, K. A., González, I. & Déjean, S. IntegrOmics: An R package to unravel relationships between two omics datasets. *Bioinformatics* **25**, 2855–2856 (2009).
104. Wickham, H. *Ggplot2: Elegant Graphics for Data Analysis*. (Springer, New York, 2016).
105. Dixon, P. VEGAN, a package of R functions for community ecology. *J. Vegetation Sci.* **14**, 927–930 (2003).
106. Li, H. & Durbin, R. Fast and accurate short read alignment with Burrows–Wheeler transform. *Bioinformatics* **25**, 1754–1760 (2009).
107. Okonechnikov, K., Conesa, A. & García-Alcalde, F. Qualimap 2: Advanced multi-sample quality control for high-throughput sequencing data. *Bioinformatics* **32**, 292–294 (2016).
108. Koboldt, D. C. et al. VarScan: Variant detection in massively parallel sequencing of individual and pooled samples. *Bioinformatics* **25**, 2283–2285 (2009).
109. Li, H. Wgsim - Read simulator for next generation sequencing. *Github repository* https://github.com/lh3/wgsim (2011).
110. Li, H. A statistical framework for SNP calling, mutation discovery, association mapping and population genetical parameter estimation from sequencing data. *Bioinformatics* **27**, 2987–2993 (2011).
111. Danecek, P. et al. The variant call format and VCFtools. *Bioinformatics* **27**, 2156–2158 (2011).
112. Bergey, C. vcf-tab-to-fasta. (2012).
113. Nguyen, L. T., Schmidt, H. A., Von Haeseler, A. & Minh, B. Q. IQ-TREE: A fast and effective stochastic algorithm for estimating maximum-likelihood phylogenies. *Mol. Biol. Evolution* **32**, 268–274 (2015).
114. Hoang, D. T. et al. UFBoot2: Improving the ultrafast bootstrap approximation. *Mol. Biol. Evolution* **35**, 518–522 (2017).
115. Olson, R. D. et al. Introducing the Bacterial and Viral Bioinformatics Resource Center (BV-BRC): A resource combining PATRIC, IRD and ViPR. *Nucleic Acids Res.* **51**, D678–D689 (2023).
116. Kumar, S., Stecher, G., Li, M., Knyaz, C. & Tamura, K. MEGA X: Molecular evolutionary genetics analysis across computing platforms. *Mol. Biol. Evolution* **35**, 1547–1549 (2018).
117. Suzek, B. E. et al. UniRef clusters: A comprehensive and scalable alternative for improving sequence similarity searches. *Bioinformatics* **31**, 926–932 (2015).
118. Caspi, R. et al. The MetaCyc database of metabolic pathways and enzymes - a 2019 update. *Nucleic Acids Res.* **48**, D445–D453 (2020).
119. Kanehisa, M., Furumichi, M., Sato, Y., Kawashima, M. & Ishiguro-Watanabe, M. KEGG for taxonomy-based analysis of pathways and genomes. *Nucleic Acids Res.* **51**, D587–D592 (2023).
120. Kanehisa, M., Sato, Y., Furumichi, M., Morishima, K. & Tanabe, M. New approach for understanding genome variations in KEGG. *Nucleic Acids Res.* **47**, D590–D595 (2019).
121. Kanehisa, M. & Goto, S. KEGG: Kyoto Encyclopedia of Genes and Genomes. *Nucleic Acids Res.* **28**, 27–30 (2000).
122. Rinke, C. et al. A standardized archaeal taxonomy for the Genome Taxonomy Database. *Nat. Microbiol.* **6**, 946–959 (2021).
123. Parks, D. H. et al. A standardized bacterial taxonomy based on genome phylogeny substantially revises the tree of life. *Nat. Biotechnol.* **36**, 996–1004 (2018).
124. Parks, D. H. et al. A complete domain-to-species taxonomy for Bacteria and Archaea. *Nat. Biotechnol.* **38**, 1079–1086 (2020).
125. Parks, D. H. et al. GTDB: An ongoing census of bacterial and archaeal diversity through a phylogenetically consistent, rank normalized and complete genome-based taxonomy. *Nucleic Acids Res.* **50**, D785–D794 (2022).
126. Pochon, Z. et al. aMeta: An accurate and memory-efficient ancient metagenomic profiling workflow. *Genome Biol.* **24**, 242 (2023).
127. Lu, J., Breitwieser, F. P., Thielen, P. & Salzberg, S. L. Bracken: Estimating species abundance in metagenomics data. *PeerJ Comput. Sci.* **3**, e104 (2017).
128. Benjamini, Y. & Hochberg, Y. Controlling the false discovery rate: A practical and powerful approach to multiple testing. *J. R. Stat. Soc., Ser. B (Stat. Methodol.)* **57**, 289–300 (1995).

Acknowledgements

We extend our deepest gratitude to the Charleston Community and the City of Charleston for supporting this work. This research was supported by the University of Pennsylvania Research Foundation (T.G.S.) and the National Science Foundation [SPRF-FR-2105384 (R.E.F.); #BCS-2045308 (C.M.L. and T.P.H.)].

Author contributions

Conceptualization: R.E.F, J.K.G., L.O., T.G.S. Formal analysis: R.E.F., T.P.H., S.J.J. Investigation: R.E.F., S.J.J., C.A.A., T.P.H, W.D.B., S.M.A. Writing—Original Draft: R.E.F., T.P.H., S.J.J. Writing—review and editing: R.E.F., T.P.H., S.J.J., C.M.L., T.G.S., J.K.G., L.O. Visualization: R.E.F., T.P.H., S.J.J. Supervision: R.E.F., T.G.S., C.M.L. Project Administration: J.K.G., L.O., A.A.O., C.A.A. Funding Acquisition: R.E.F., T.P.H., C.M.L., T.G.S.

Competing interests

The authors declare no competing interests.

Additional information

Supplementary information The online version contains supplementary material available at https://doi.org/10.1038/s42003-024-06893-0.

Correspondence and requests for materials should be addressed to Raquel E. Fleskes, Cecil M. Lewis or Theodore G. Schurr.

Peer review information *Communications Biology* thanks Maria Ávila-Arcos and the other, anonymous, reviewers for their contribution to the peer review of this work. Primary Handling Editor: Tobias Goris. A peer review file is available.